Polymer 50 (2009) 57–67

Contents lists available at ScienceDirect

Polymer

journal homepage: www.elsevier.com/locate/polymer

An argon laser induced polymerization photoinitiated by both mono- and bichromophoric hemicyanine dye–borate salt ion pairs. The synthesis, spectroscopic, electrochemical and kinetic studies

Janina Kabatc [a,*], Agnieszka Celmer [b]

[a] University of Technology and Life Sciences, Faculty of Chemical Technology and Engineering, Seminaryjna 3, 85-326 Bydgoszcz, Poland
[b] Master Degree Student at Faculty of Chemical Technology and Engineering, University of Technology and Life Sciences, Bydgoszcz, Poland

ARTICLE INFO

Article history:
Received 17 April 2008
Received in revised form
22 October 2008
Accepted 27 October 2008
Available online 30 October 2008

Keywords:
Dyeing photoinitiators
Bichromophoric dye
Radical polymerization

ABSTRACT

A series of homodimeric hemicyanine dyes based on (*p*-dimethylaminostyryl)benzothiazolium, (*p*-dimethylaminostyryl)benzoxazolium, (*p*-dimethylaminostyryl)-2,3,3-trimethyl-3*H*-indolium residues were synthesized. Several photoredox pairs containing mono- and bichromophoric hemicyanine dyes, possessing benzothiazole, benzoxazole or indolinium group linked by 5 or 10 methylene groups have been evaluated as novel photoinitiators for free radical polymerization induced with the argon-ion laser visible emission. In tested photoredox pairs, hemicyanine dye acts as an electron acceptor and it is coupled with borate anion which is an electron donor. The photochemistry of the series of bichromophoric hemicyanine borates: 1,5-bis-[*N*,*N*′-(2,2′-(4-*N*,*N*-dimethylamino)styryl)benzothiazolium]pentane, 1,10-bis-[*N*,*N*′-(2,2′-(4-*N*,*N*-dimethylamino)styryl)benzothiazolium]decane (**S5**, **S10**), 1,5-bis-[*N*,*N*′-(2,2′-(4-*N*,*N*-dimethylamino)styryl)benzoxazolium]pentane, 1,10-bis-[*N*,*N*′-(2,2′-(4-*N*,*N*-dimethylamino)styryl)benzoxazolium]decane (**O5**, **O10**) and 1,5-bis-[*N*,*N*′-(2,2′-(4-*N*,*N*-dimethylamino)styryl)-3,3,3′,3′-tetramethyl-3*H*-indolium]pentane, 1,10-bis-[*N*,*N*′-(2,2′-(4-*N*,*N*-dimethylamino)styryl)-3,3,3′,3′-tetramethyl-3*H*-indolium]decane (**I5**, **I10**) was compared to the photochemistry of structurally related monochromophoric hemicyanine borates (**S1**, **O1**, **I1**).

1. Introduction

Polymer photoinitiating systems introduced by Dupont in the 50s [1] are an important application of photochemical technology [2]. Polymerization reaction can be carried out in an image forming fashion. They can form a pattern as a thin film or can form layers [3–5].

The photoinitiator system generates the free radicals that initiate radical chain polymerization of an unsaturated monomer. It may be a single compound, typically called a photoinitiator rather than a photoinitiator system that absorbs light and undergoes unimolecular reaction to form radicals. It may consist, as well, several different compounds that undergo a complex series of consecutive reactions to produce the initiating radicals [6].

The photoinitiator system is a formulation, composition of which depends on an application [3–5].

There are many examples of application of dyes as photoinitiators. These include photoreducible dyes: xanthene and acridine dyes which can directly photoinitiate polymerization of methyl

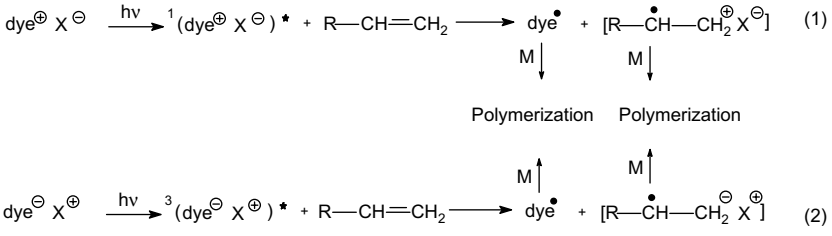

methacrylate, styrene and acrylonitrile, with low efficiency [2,7,8]. Photoinitiation occurs by electron transfer between the singlet excited dye molecule and monomer (Eqs. (1) and (2)). Electron deficient monomers (like acrylates) react preferentially as electron

* Corresponding author. Tel.: +48 52 374 9064; fax: +48 52 374 9009.
E-mail address: nina@utp.edu.pl (J. Kabatc).

0032-3861/$ – see front matter © 2008 Elsevier Ltd. All rights reserved.
doi:10.1016/j.polymer.2008.10.036

acceptors, whereas polymerization of electron rich monomers occurs by monomer oxidation [2,5].

As it was mentioned above the photoinitiation of polymerization usually does not occur upon interaction of the excited singlet or triplet state of dye with monomer molecule [2]. Therefore, in most practical applications of photoinduced radical polymerization, the sensitizers are UV-absorbing compounds that undergo unimolecular fragmentation in an excited state to form the initiating radicals. It has been proven difficult to extend this concept very far into the visible region of the spectrum. Most of the useful initiating systems that respond to visible light are based on quite different, usually bimolecular chemistry. For example, a sensitization, in order to be useful in the blue region, involves a bimolecular electron-transfer reaction between an excited chromophore and an electron molecule compound to form, in the case of neutral reactants, a radical anion and the radical cation. Subsequent proton transfer or other types of consecutive reaction result in radicals that are capable of initiating polymerization [9]. Such approach is the most promising systems offering further extension of the photoresponse into visible region.

Two types of sensitization of free radical polymerization can occur:

1. Photoreducible dye sensitization reported first by Oster in 1954 [10]. Oster identified several groups of effective dyes, which are photoreduced in the presence of co-initiator (electron donor).
2. Photooxidizable dye sensitization. Photooxidation of a dye ($dye^{+}X^{-}$, electron donor) in the presence of co-initiator (electron acceptor) is a good example of such type photoinitiating system [2,9].

Initiation of polymerization by photoreducible dyes in the presence of different co-initiators (electron donors) is very common, whereas a polymerization initiated by photooxidation of dye in the presence of an electron acceptor is rather rare. For example, thiazine dyes such as Methylene blue can react either as electron acceptor in the presence of *N*-phenylglycine [11], or as electron donor in the presence of benzyltrimethylstannane being the electron acceptor [2,12].

The secondary reaction following electron transfer process involves either the proton transfer or the fragmentation reaction (cleavage). The second type of reaction can occur as reductive cleavage (Eq. (3)) or as oxidative cleavage (Eq. (4)), depending on whether the compound that undergoes the cleavage reaction has been initially reduced or oxidized. Here, D^{*} represents an excited state of an electron donor, A^{*} represents an excited state of an electron acceptor and X–Y is the compound that undergoes cleavage. When the X–Y molecule is charged, the most likely photoinduced electron-transfer reaction is either reduction if the molecule is a cation or oxidation if the molecule is an anion. Both processes form a neutral radical, $X–Y^{\bullet}$. In these cases, fragmentation of the $X–Y^{\bullet}$ yields a radical, $X^{\bullet}$, and a neutral species Y [9].

$$D^{*} + X{-}Y^{+} \rightarrow D^{\bullet+} + X{-}Y^{\bullet} \rightarrow X^{\bullet} + Y \quad (3)$$

$$A^{*} + X{-}Y^{-} \rightarrow A^{\bullet-} + X{-}Y^{\bullet} \rightarrow X^{\bullet} + Y \quad (4)$$

A number of examples of reductive cleavage of cationic acceptors (Eq. (3)) and oxidative cleavage of anionic donors (Eq. (4)) have been reported [9].

For most cases photoreducible dyes have maximum absorption in a visible light spectrum. A suitable dye/co-initiator system must first exhibit a high absorption in the wavelength delivered by visible light sources (lasers) and, secondly, efficiently generate the reactive initiating radicals [9].

The well known examples of photoinitiating systems are cation–anion couples: cyanine dye/borate salt. The cyanine dyes act as a visible light absorber in many photoinitiator systems.

The ion pair composed of cyanine dye cation and an alkyltriarylborate anion was first described by Schuster et al. [13,14]. Their work [14] on the photochemistry of cyanine borates led to the preparation of the color-tunable, operating in the visible region commercial photoinitiators [15]. According to this study, the initiation step of the reaction involves alkyl radical formation as a result of photoinduced electron transfer from borate anion to the excited singlet state of cyanine dye, followed by the rapid cleavage of the carbon–boron bond of the boranyl radical.

From our studies it is known that for cyanine borate salts in some cases there is a direct relationship between the rate of free radical polymerization and the rate of electron transfer process. On the other hand, the efficiency of electron transfer process depends on the distance between an electron acceptor and an electron donor. Since the lifetime of the excited singlet state of cyanine dye is very short (about or less than 1 ns), therefore the formation of the tight ion pair increases the efficiency of electron transfer process. In the simplest way, the formation of contact ion pair can be enhanced by an increase of electron donor ion concentration (co-initiator). It is worth noting that for the cyanine borate salts, the influence of an additional amount of borate anion on the rate of photoinitiated polymerization depends on a dye cation type. The results obtained in our laboratory suggest that the borate cyanine salts in the tested polymerizable formulation exist as tight ion pair only at about 40–50% [16,17]. The more advance method considers an increase of an electron donor concentration in proximity to the absorbing dye exclusively by a coupling of electron donor. In the case of cyanine–borate couple it is possible by adding an additional organic cation capable of an ion pair formation with borate ion in proximity to the absorbing dye [16–18]. The experimental results evidently have shown that such approach increases a co-initiator concentration in the close neighbourhood to the absorbing dye that is demonstrated by an increase of the rate of polymerization, and strong deviation from linear Stern–Volmer relationship describing the kinetics of quenching of excited sensitizer by electron donor [16,18].

In this paper, we describe the synthesis, spectroscopic, electrochemical and kinetic studies of the novel photoinitiating systems consisting different bichromophoric hemicyanine dyes (the light absorbers) coupled with *n*-butyltriphenylborate anions (co-initiators). The photoinitiating ability of the tested photoredox systems is compared to the photochemistry of structurally related, monochromophoric hemicyanine borate salts. Additionally, it is our intention to show that the Marcus equation can be applied for the description of the kinetics for dye–borate photoinitiated polymerization *via* an intermolecular electron transfer process.

2. Experimental

2.1. Materials

2-Metylbenzothiazole, 2-methylbenzoxazole, 2,3,3-trimethylindolenine, 1,5-diiodopentane, 1,10-diiododecane, 4-(*N*,*N*-dimethylamino)benzaldehyde and solvents were obtained from Aldrich Chemical Co. Used as co-initiator *n*-butyltriphenylborate tetramethylammonium salt (B2) was synthesized based on the method described by Damico [19]. 2-Ethyl-2-(hydroxymethyl)-1,3-propanediol triacrylate (TMPTA) and 1-methyl-2-pyrrolidinone (MP) were purchased from Aldrich and were used as monomer and solvent, respectively.

2.2. Measurements

(i) All final products of synthesis were identified by ^{1}H and ^{13}C NMR spectroscopy. The spectra obtained were the evidence

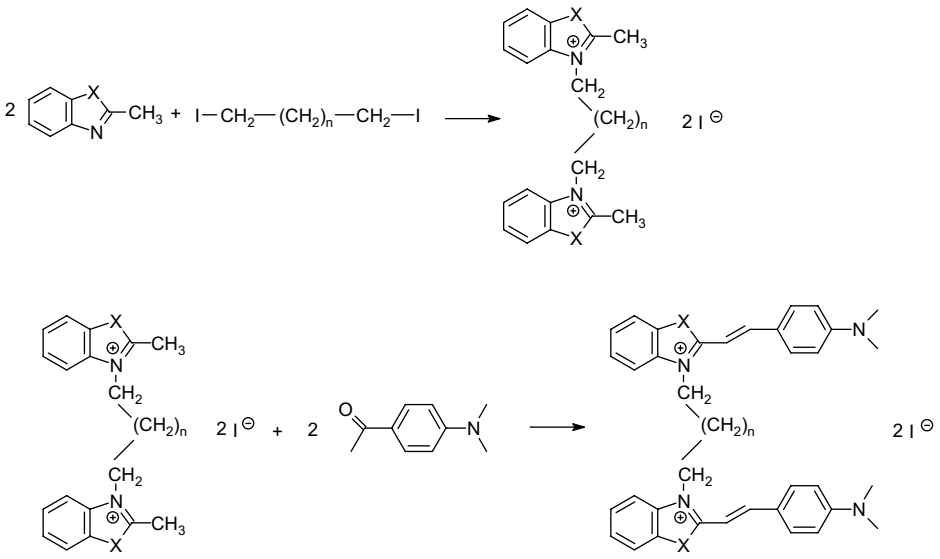

Scheme 1.

that the reaction products were of the desired structures. The purity of synthesized compounds was determined using a thin layer chromatography and by measuring the melting points. The purities of the dyes were as it is required for the spectroscopic studies.

The ^{1}H and ^{13}C NMR spectra were recorded with the use of a Varian spectrometer Gemini 200 operating at 200 MHz. Dimethylsulfoxide (DMSO) was used as solvent and tetramethylsilane (TMS) as internal standard.

The elemental analysis was made with a Vario MACRO 11.45-0000, Elementar Analysensysteme GmbH (Germany), operating with the software VARIOEL 5.14.4.22.

Melting points (uncorrected) were determined on the Boëthius apparatus – PGH Rundfunk, Fernsehen Niederdorf KR, Stollberg/E.

(ii) Spectroscopic measurements: UV–vis absorption spectra were obtained using Shimadzu UV–vis Multispec-1500 Spectrophotometer, and steady-state fluorescence using a Hitachi F-4500 Spectrofluorimeter.

(iii) The reduction and oxidation potentials of dyes and *n*-butyltriphenylborate salt were measured by cyclic voltammetry. An Electroanalytical MTM System model EA9C-4z (Cracow, Poland), equipped with a small-volume cell was used for the measurements. A 1 mm platinum disc electrode was used as the working electrode. A Pt wire constituted the counter electrode, and an Ag–AgCl electrode served as the reference electrode. The supporting electrolyte was 0.1 M tetrabutylammonium perchlorate in dry acetonitrile. The solution was degassed by bubbling argon gas through the solution. The potential was swept from −1.6 to 1.6 V with the sweep rate of 500 mV/s to record the current–voltage curve.

(iv) Photoinitiated polymerization rate (R_p) profiles were determined by a differential scanning calorimetry (DSC), under isothermal conditions at room temperature using a photo-DSC apparatus constructed on the basis of a TA Instruments DSC 2010 Differential Scanning Calorimeter. The 40 mg of sample was polymerized in open aluminium pans having the diameter of 6.6 mm. The irradiation of the polymerization mixture was carried out using the visible emission (514 nm) of an argon-ion laser (Melles Griot). The average power of irradiation was 20 mW/0.196 cm^2 at 514 nm.

A polymerization solution was composed of 1 ml of 1-methyl-2-pyrrolidinone (MP) and 9 ml of 2-ethyl-2-(hydroxymethyl)-1,3-propanediol triacrylate (TMPTA). The co-initiator concentration used in experiments was 2×10^{-3} M and dye concentration was 2×10^{-3} M per one-chromophore. As a reference sample, a polymerizing mixture containing cyanine iodides (dye without a co-initiator) was used. The polymerizing mixture was not deaerated. In order to reduce the effect of diffusion-controlled termination, the effect of a network formation, the Norrish–Troomsdorf effect and radicals trapping effect, the initial rates of polymerization were taken into account for further consideration. The initial rates of polymerization are the slopes of the lines drawn on the flow of heat versus time curve at the initial time of polymerization.

2.3. Synthesis

The synthetic approaches applied are outlined below and are based on the condensation reaction of 1,5-bis-[*N*,*N*′-(2-methylbenzothiazolium)pentane diiodide, 1,5-bis-[*N*,*N*′-(2-methylbenzoxazoium)pentane diiodide, 1,5-bis-[*N*,*N*′-(2,3,3-trimethyl-3*H*-indolium)pentane diiodide, 1,10-bis-[*N*,*N*′-(2-methylbenzothiazolium)-decane diiodide, 1,10-bis-[*N*,*N*′-(2-methylbenzoxazolium)decane diiodide and 1,10-bis-[*N*,*N*′-(2,3,3-trimethyl-3*H*-indolium)decane diiodide (**SL5**, **SL10**, **OL5**, **OL10**, **IL5**, **IL10**) with *p*-(*N*,*N*-dimethylamino)benzaldehyde.

A general route for the synthesis of homobicationic hemicyanine dyes is shown in Scheme 1.

As it is shown in Scheme 1 the synthesis of the bichromophoric hemicyanine dyes undergoes *via* two steps:

- The quaternization reaction of 2-methylbenzothiazole, 2-methylbenzoxazole and 2,3,3-trimethylindolenine with 1,5-diiodopentane or 1,10-diiododecane yielding corresponding diheterocyclic salts (**SL5**, **SL10**, **OL5**, **OL10**, **IL5**, **IL10**).
- The condensation reaction of diheterocyclic salts (**SL5**, **SL10**, **OL5**, **OL10**, **IL5**, **IL10**) with *p*-(*N*,*N*-dimethylamino)benzaldehyde yielding the corresponding bichromophoric hemicyanine dye (**S5**, **S10**, **O5**, **O10**, **I5**, **I10**).

The synthesis of monochromophore dyes was described in our papers [16,17] and their structures are presented below:

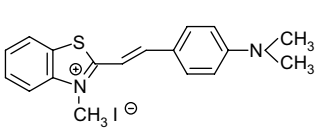

S1

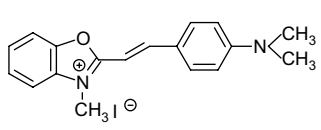

O1

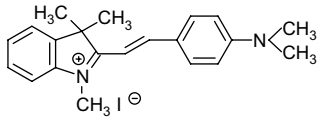

I1

*2.3.1. General procedure for the synthesis of quaternary salts of applied heterocycles (**SL5**, **SL10**, **OL5**, **OL10**, **IL5**, **IL10**)*

A mixture of 0.011 mol of corresponding heterocycle and 0.005 mol α,ω-dihalogenalkane in 5 ml of dioxane was boiled for 6 h. Obtained salt was precipitated by diethyl ether and filtered off. The product was washed with isopropanol and ether. Quaternary salts were used in next steps of synthesis without additional purification [20].

*2.3.2. General procedure for the synthesis of bichromophoric styrylcyanine dyes (**S5**, **S10**, **O5**, **O10**, **I5**, **I10**)*

A mixture of 0.001 mol of diquaternary salt and 0.002 mol of *p-(N,N*-dimethylamino)benzaldehyde in 3 ml of acetic anhydride was boiled for 10 min. Obtained crude dye was precipitated by diethyl ether and filtered off. Precipitate was washed with alcohol and crystallized from DMF–methanol mixture [20].

*2.3.2.1. Dye **S5** – 1,5-bis-[*N,N′*-(2,2′-(4*-N,N-*dimethylamino)styryl)-benzothiazolium]pentane diiodide.* The dye was prepared by the procedure described above using 1,5-bis-[*N,N′*-(2-methylbenzothiazolium)pentane diiodide (0.003 mol, 1.87 g) and *p-(N,N*-dimethylamino)benzaldehyde (0.006 mol, 0.9 g) in 9 ml of acetic anhydride. The dark green solid obtained was crystallized from DMF/methanol mixture; 2.44 g, yield 91.83%.

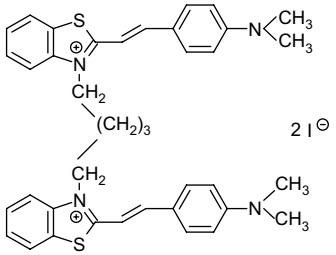

*2.3.2.2. Dye **O5** – 1,5-bis-[*N,N′*-(2,2′-(4*-N,N-*dimethylamino)styryl)-benzoxazolium]pentane diiodide.* The dye was synthesized by applying the methodology described for **S5** using 1,5-bis-[*N,N′*-(2-methylbenzoxazolium)pentane diiodide (0.003 mol, 1.77 g) and *p-(N,N*-dimethylamino)benzaldehyde (0.006 mol, 0.9 g) in 9 ml of acetic anhydride as substrates. The crude dark blue solid was crystallized from DMF/methanol mixture; 1.52 g, yield 59.46%.

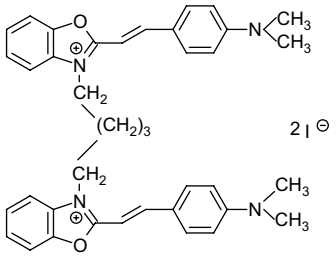

*2.3.2.3. Dye **I5** – 1,5-bis-[*N,N′*-(2,2′-(4*-N,N-*dimethylamino)styryl)-3,3,3′,3′-tetramethyl-*3H*-indolium]pentane diiodide.* The dye was prepared according the procedure described above using as substrates 1,5-bis-[*N,N′*-(2,3,3-trimethylindolinium)pentane diiodide (0.003 mol, 1.89 g) and *p-(N,N*-dimethylamino)benzaldehyde (0.006 mol, 0.9 g) in 9 ml of acetic anhydride. The gold-green solid obtained was crystallized from DMF/methanol mixture; 2.22 g, yield 81.86%.

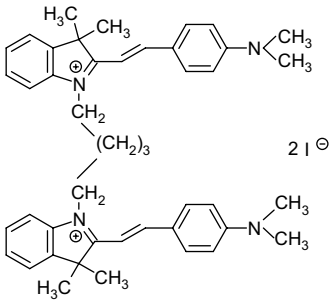

*2.3.2.4. Dye **S10** – 1,10-bis-[*N,N′*-(2,2′-(4*-N,N-*dimethylamino)styryl) benzothiazolium]decane diiodide.* This dye was prepared by applying the procedure described above using 1,10-bis-[*N,N′*-(2-methylbenzothiazolium)decane diiodide (0.003 mol, 2.08 g) and *p-(N,N*-dimethylamino)benzaldehyde (0.006 mol, 0.9 g) in 9 ml of acetic anhydride. The purple solid was obtained and crystallized from DMF/methanol mixture; 1.87 g, yield 65.21%.

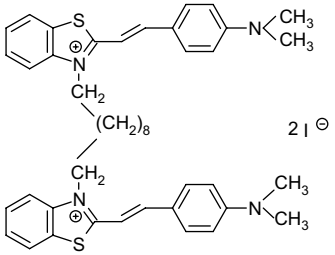

*2.3.2.5. Dye **O10** – 1,10-bis-[*N,N′*-(2,2′-(4*-N,N-*dimethylamino)styryl)-benzoxazolium]decane diiodide.* The dye was prepared based on the procedure described above using 1,10-bis-[*N,N′*-(2-methylbenzoxazolium)decane diiodide (0.003 mol, 1.98 g) and *p-(N,N*-dimethylamino)benzaldehyde (0.006 mol, 0.9 g) in 9 ml of acetic anhydride. The dark blue solid obtained was crystallized from DMF/methanol mixture; 2.25 g, yield 81.34%.

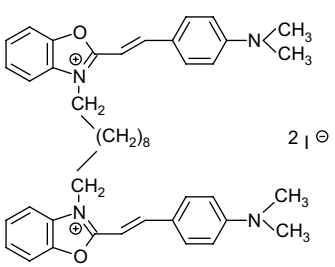

*2.3.2.6. Dye **I10** – 1,10-bis-[*N,N′*-(2,2′-(4*-N,N-*dimethylamino)styryl)-3,3,3′,3′-tetramethyl-*3H*-indolium]decane diiodide.* The dye was prepared according the procedure described above using 1,10-bis-[*N,N′*-(2,3,3-trimethylindolium)decane diiodide (0.003 mol, 2.10 g) and *p-(N,N*-dimethylamino)benzaldehyde (0.006 mol, 0.9 g) in 9 ml

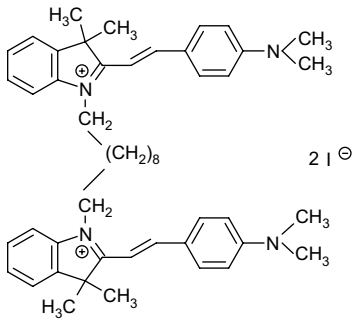

of acetic anhydride. The gold-green solid was obtained and was purified by crystallization from DMF/methanol mixture; 2.02 g, yield 69.13%.

3. Results and discussion

3.1. Molecular design and synthetic procedures

Six, possessing two identical chromophores, dyes have been synthesized by the reaction of appropriate diheterocyclic diiodides by Knoevenagel condensation with proper *p*-(*N*,*N*-dimethylamino)benzaldehyde (Scheme 1). To obtain quaternary salts, which are precursors for the bichromophoric dyes, corresponding heterocycle (2-methylbenzothiazole, 2-methylbenzoxazole, 2,3,3-trimethylindolenine) was boiled in dioxane with appropriate α,ω-dihalogenalkane. *p*-(*N*,*N*-dimethylamino)benzaldehyde was added to the yielded quaternary salts and the mixture was boiled in acetic anhydride similarly as described in Ref. [20]. Details of the synthetic procedures and structures of obtained dyes (see Scheme 1) are described in Section 2. The dyes were purified by crystallization from DMF/methanol mixture. The structures and purities of the prepared compounds were confirmed by ^{1}H and ^{13}C NMR spectroscopy, elementary analysis and thin layer chromatography. The data of the analysis for all dyes are given in Table 1.

The length of the link between two hemicyanine chromophores (5 or 10 methylene groups) differentiates the six dimers (named **S5**, **S10**, **O5**, **O10**, **I5** and **I10**).

It is noteworthy that the ^{1}H NMR spectra (Table 1) display two characteristic doublets localized at chemical shifts in the range of 7–8 ppm. They are attributed to both vinyl hydrogen atoms. Based on the large coupling for the olefinic protons ($J = 15$–16 Hz) it is concluded that these dyes exist as *all-trans* conformation in the ground state.

3.2. Spectroscopic studies

The electronic absorption spectra of selected bichromophoric dyes in *N*,*N*-dimethylformamide are shown in Fig. 1.

Spectral properties of bichromophoric styrylcyanine dyes and their corresponding monochromophoric analogs in both *N*,*N*-dimethylformamide (DMF) and tetrahydrofurane (THF) are presented in Table 2.

All electronic absorption spectra in polar solvents present two bands whose maxima are located at about 300 and 550 nm regions. The shortest wavelength bands are attributed to the $\pi \rightarrow \pi^*$ transitions whereas the long wavelength bands, generally characterized by higher molar absorption coefficients, are attributed to the $S^0 \rightarrow$ CT transition. The $S^0 \rightarrow$ CT transition is caused by an intramolecular charge transfer transition (ICT) involving electron lone pair of the amino nitrogen and the cationic benzothiazolium, benzoxazolium or indolinium nitrogen moiety [21,22]. Inspection of the illustrative absorption spectra, presented in Fig. 1, shows that the position and

Table 1
Characteristics of the bichromophoric styrylcyanine dyes tested.

Dye	Empirical formula	Molecular mass [g/mol]	M.p. [°C]	^{1}H NMR (DMSO-d_6) δ (ppm)	^{13}C NMR (DMSO-d_6) δ (ppm)	Elemental analysis
S5	$C_{39}H_{42}S_2N_4I_2$	884	215	1.498 (m, 2H), 1.813–1.952 (m, 4H), 3.135 (s, 12H, N–$(CH_3)_2$), 4.776 (m, 4H), 6.791–6.831 (d, 2H, $J = 8$ Hz), 7.465–7.542 (d, 2H, $J = 15.4$ Hz), 7.571–7.593 (m, 4H), 7.630–7.703 (m, 4H), 7.791–7.868 (d, 2H, $J = 15.4$ Hz), 7.948–7.998 (d, 2H), 8.033–8.058 (d, 2H), 8.278–8.318 (d, 2H)	21.116, 27.329, 28.035, 32.222, 47.734, 63.528, 105.644, 111.857, 115.907, 123.933, 127.415, 128.955, 133.036, 150.552	Anal. calcd. for $C_{39}H_{42}S_2N_4I_2$: C, 52.94%; H, 4.75%; N, 6.33%. Found: C, 49.76%; H, 4.447%; N, 6.217%
S10	$C_{44}H_{52}S_2N_4I_2$	954	178	1.212–1.260 (m, 12H), 1.644–1.897 (m, 4H), 3.11 (s, 12H, N–$(CH_3)_2$), 4.652–4.835 (m, 4H), 6.754–6.860 (d, 4H), 7.567–7.648 (d, 2H, $J = 16.2$ Hz), 7.666–7.707 (t, 2H), 7.736–7.773 (t, 4H), 7.791–7.827 (d, 2H), 7.835–7.886 (m, 2H), 8.285–8.344 (d, 2H), 8.425–8.457 (d, 2H)	21.193, 25.705, 27.867, 28.891, 29.824, 32.859, 47.969, 51.436, 60.721, 105.788, 111.902, 115.983, 124.024, 127.453, 128.978, 131.567, 133.036, 150.506	Anal. calcd. for $C_{44}H_{52}S_2N_4I_2$: C, 55.34%; H, 5.45%; N, 5.87%. Found: C, 57.35%; H, 4.895%; N, 5.536%
O5	$C_{39}H_{42}O_2N_4I_2$	852	165	1.505–1.542 (m, 2H), 1.762–1.897 (m 4H), 3.121 (s, 12H, N–$(CH_3)_2$), 4.556–4.586 (m, 4H), 6.798–6.871 (t, 2H), 7.318–7.399 (d, 2H, $J = 16.2$ Hz), 7.593–7.699 (m, 4H), 7.820–8.194 (m, 10H), 8.216–8.293 (d, 2H, $J = 15.4$ Hz)	22.891, 26.904, 32.024, 32.358, 39.853, 44.829, 60.448, 96.116, 111.075, 113.594, 119.473, 127.059, 128.788, 133.241, 151.606	Anal. calcd. for $C_{39}H_{42}O_2N_4I_2$: C, 54.93%; H, 4.93%; N, 6.57%. Found: C, 54.40%; H, 4.474%; N, 6.133%
O10	$C_{44}H_{52}O_2N_4I_2$	922	125	1.179–1.322 (m, 12H), 1.806–1.897 (m 4H), 3.11 (s, 12H, N–$(CH_3)_2$), 4.542 (m, 4H), 6.758–6.842 (d, 4H), 7.051–7.121 (d, 2H, $J = 14$ Hz), 7.282–7.384 (m, 4H), 7.615–7.686 (d, 2H, $J = 15.4$ Hz), 7.895–7.919 (m, 2H), 7.937–8.011 (m, 4H), 8.190–8.278 (m, 2H)	21.960, 25.829, 26.345, 27.324, 28.219, 28.864, 39.826, 45.068, 46.949, 96.246, 111.116, 112.011, 113.589, 116.684, 119.544, 127.078, 129.801, 133.230, 151.574	Anal. calcd. for $C_{44}H_{52}O_2N_4I_2$: C, 57.27%; H, 5.64%; N, 6.07%. Found: C, 52.82%; H, 5.219%; N, 5.508%
I5	$C_{45}H_{54}N_4I_2$	904	172	1.209 (m, 6H), 1.740 (s, 12H), 3.141 (s, 12H, N–$(CH_3)_2$), 4.447 (m, 4H),, 6.849–6.886 (d, 4H), 7.186–7.263 (d, 2H, $J = 15.4$ Hz), 7.421–7.523 (t, 4H), 7.659–7.692 (d, 2H), 7.754–7.784 (d, 2H), 8.047–8.008 (d, 4H), 8.289–8.366 (d, 2H, $J = 15.4$ Hz)	15.199, 20.805, 21.161, 26.707, 27.852, 45.072, 53.978, 60.372, 93.590, 104.445, 111.068, 112.190, 113.654, 122.742, 127.423, 128.735, 134.591, 154.541	Anal. calcd. for $C_{45}H_{54}N_4I_2$: C, 59.73%; H, 5.97%; N, 6.19%. Found: C, 54.97%; H, 5.854%; N 5.973%
I10	$C_{50}H_{64}N_4I_2$	974	125	1.406 (m, 8H), 1.658 (s, 12H), 1.852–1.884 (m, 8H), 3.169 (s, 12H, N–$(CH_3)_2$), 4.493 (m, 4H), 6.793–6.839 (d, 4H), 7.101–7.180 (d, 2H, $J = 15.8$ Hz), 7.376–7.449 (t, 4H), 7.605–7.636 (d, 4H), 7.678–7.720 (d, 2H), 7.953–7.999 (d, 2H), 8.160–8.237 (d, 2H, $J = 15.4$ Hz)	14.228, 21.131, 22.079, 25.887, 27.314, 28.853, 28.709, 40.004, 45.004, 47.666, 63.528, 104.635, 112.243, 113.685, 122.894, 127.551, 128.849, 129.448, 134.371, 154.496	Anal. calcd. for $C_{50}H_{64}N_4I_2$: C, 61.60%; H, 6.57%; N, 5.75%. Found: C, 57.56%; H, 5.853%; N, 5.190%

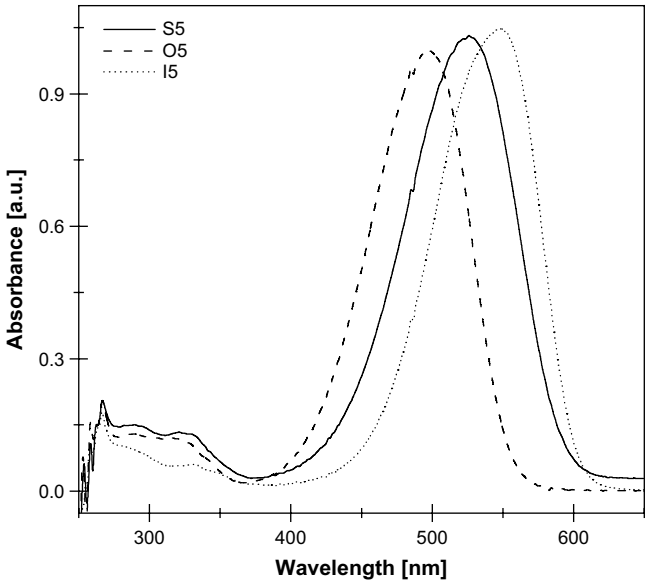

Fig. 1. Electronic absorption spectra of selected bichromophoric dyes in *N*,*N*-dimethylformamide at 293 K. The chromophores possess different acceptor groups (dye marked in the figure).

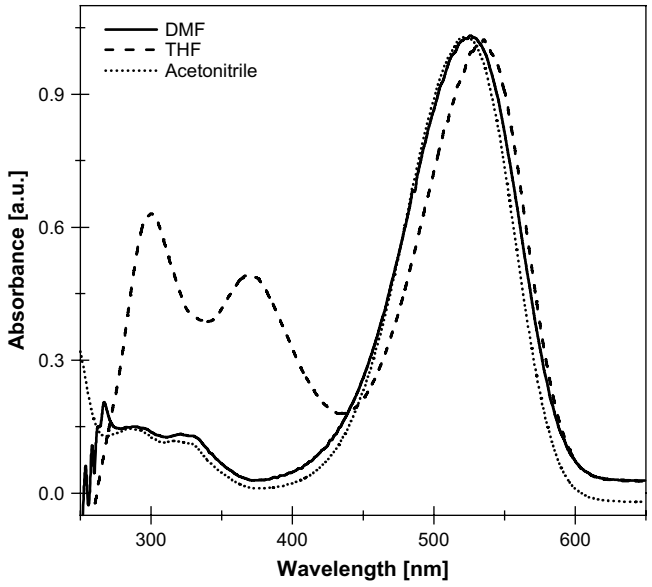

Fig. 2. Representative electronic absorption spectra of the **S5** dye. Spectra recorded in *N*,*N*-dimethylformamide (DMF), tetrahydrofurane (THF) and acetonitrile at 293 K.

intensity of CT absorption band depend on the type of heterocyclic ring. The molar absorption coefficient of tested dyes is about twice as high as measured for their monomeric equivalents.

Figs. 2 and 3 show the absorption and fluorescence spectra of **S5** and **O5** dyes in three different, common solvents: *N*,*N*-dimethylformamide, tetrahydrofurane and acetonitrile, respectively. Generally speaking, the polarities of these solvents are in the following order: *N*,*N*-dimethylformamide > acetonitrile > tetrahydrofurane.

It has been established experimentally that the molecules with π-electrons, for which the charge distribution in the electronic ground state is considerably different from that in the excited state exhibit pronounced solvatochromism. Thus, for the tested organic compounds only a comparatively small solvent dependence of their UV–vis absorption spectra is observed. A solvent change from tetrahydrofurane to *N*,*N*-dimethylformamide causes a hypsochromic shift of CT absorption band of only ca. 10 nm (355 cm^{-1}). For example, the maximum absorption peak for **S5** is observed at 536 nm in tetrahydrofurane and 526 nm in *N*,*N*-dimethylformamide, respectively. Table 2 reveals that the long wavelength absorption band undergoes a hypsochromic shift (absorption peak positions blue-shift) as the solvent polarity increases (negative solvatochromism), indicating that the ground state has larger dipole moments than excited state (Franck–Condon region) [23].

It was also observed that the monochromophoric dye (**S1**) 4-(*p*-(*N*,*N*-dimethylamino)styryl)benzothiazolium iodide shows in DMF λ_{max} at 525 nm, and its bichromophoric equivalents (**S5** and **S10**) show absorption maximum only slightly shifted to the red, e.g. at 526 and 527 nm, respectively.

Absorption maxima of bichromophoric dyes **S5**, **S10**, **O5**, **O10**, **I5** and **I10** with long methylene chain spacer (5 or 10 carbon atoms) in

Table 2
Spectroscopic properties of the mono- and bichromophoric styrylcyanine dyes in *N*,*N*-dimethylformamide (DMF) and tetrahydrofurane (THF).

Dye	$\lambda_{ab\ max}$ [nm] (ε [$M^{-1}\,cm^{-1}$])	$Ab_{v/2}$ [cm^{-1}]	$\lambda_{fl.max}$ [nm]	$Fl_{v/2}$ [cm^{-1}]	Stokes shift [cm^{-1}]
N,*N*-dimethylformamide ($\varepsilon = 36.71$, $n_D = 1.4305$)					
S1	525, (45 100)	2572	606	1197	2535
S5	526, (84 400)	2776	614	1302	2715
S10	527, (87 000)	2782	611	1326	2621
O1	498, (47 800)	2658	559	1300	2200
O5	499, (88 000)	2809	574	1443	2656
O10	497, (90 000)	2816	573	1419	2643
I1	545, (56 700)	2274	598	1282	1617
I5	548, (100 000)	2377	616	1331	1699
I10	547, (114 100)	1892	612	1348	1687
Tetrahydrofurane ($\varepsilon = 7.58$, $n_D = 1.4072$)					
S1	527, (53 600)	2476	600	1215	2308
S5	536	2502	604	1285	2115
S10	536	2502	602	1314	2080
O1	500	2658	562	1310	2200
O5	496	2690	565	1430	2484
O10	496	2643	564	1469	2422
I1	552	2300	595	1998	1301
I5	558	1858	604	1335	1430
I10	558	2322	608	1321	1819

$Ab_{v/2}$ – absorption full width at half maximum, $Fl_{v/2}$ – fluorescence full width at half maximum.

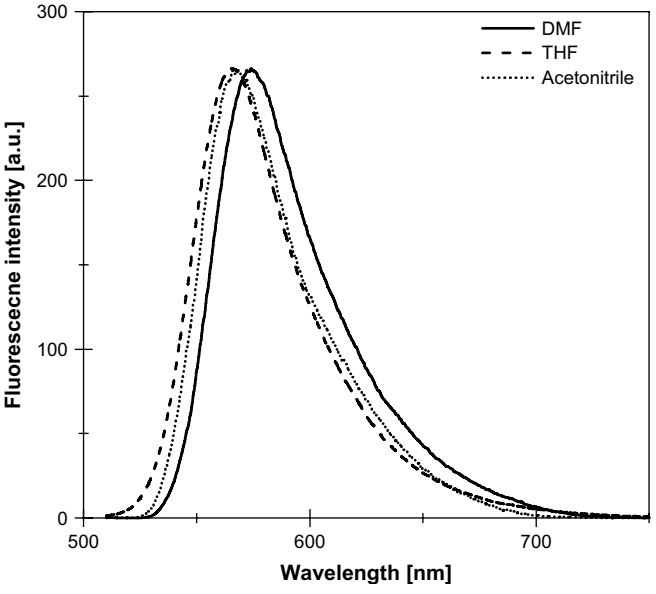

Fig. 3. Representative fluorescence spectra of the **O5** dye. Spectra recorded in *N*,*N*-dimethylformamide (DMF), tetrahydrofurane (THF) and acetonitrile at 293 K.

DMF are red-shifted only about 1–2 nm in comparison to their parent monomers. This indicates an absence of any interaction between chromophores forming bichromophoric dye in their ground state.

Generally, the absorption spectra show the negative solvatochromic behavior. The shapes of all spectra recorded for tested dyes are similar in all solvents applied, except tetrahydrofurane (THF), whose spectra is shown in Fig. 2. The spectra of hemicyanine dyes possessing two chromophores in THF as a solvent have evident absorption bands around 300 and 380 nm, which are very different from the absorption band around 500 nm. According to Huang's studies [23] on the photochemistry of similar hemicyanine dyes (styrylpyridinium), one can conclude that the absorption band at 370 nm can be assigned as a transition between the ground state of hemicyanine aggregates, whereas the 300 nm absorption is the $S_0 \rightarrow S_2$ ($\pi \rightarrow \pi^*$) transition [23–25].

It is known that the macroscopic properties of bichromophoric compounds, such as absorption, emission, strongly depend on the interaction between the different chromophores, not just the individual or isolated molecule. The most common spectroscopic behavior of aggregate is the shift of the absorption peak. The blue-shift is due to the formation of H-aggregate while red-shift due to the J-aggregate. The formation of aggregates can be tuned by external environments and an "intramolecular aggregate" can also be generated by joining two chromophores with a proper linkage [23,24,26,27].

It has been confirmed by Huang that the H-aggregate has an absorption peak around 350 nm and that the formation of H-aggregate strongly depends on experimental environments [23,24].

Hence, the strong absorption at 370 nm observed for tested dyes in THF solution is evidently a result of the formation of the H-aggregates in this solvent. Based on Huang's studies [23], there is the relationship between the formation of an aggregate and the properties of the solvents. Tetrahydrofurane has the minor polarity. Huang concludes that the possible reason for this phenomenon might be the high dipole moments of the hemicyanine chromophore: weaker polar solvents do not favor the high polar solute molecule. Thus, those high polar hemicyanine molecules are not well "dissolved" in weak polar solvents, but prefer to disperse in to aggregates [23]. Our results shown that the solubility of bichromophoric dyes in such weak polar solvents is extremely small.

The similarity between the absorption spectra of mono- and bichromophoric dyes under studies implies that the formation of aggregates is mainly controlled not by the intermolecular interaction between the solute molecules (chromophore) but by the interaction between the solute molecule and surrounding solvent molecules. Our results are similar to those obtained by Huang et al. [23,24] for styrylpyridinium dyes and clearly show that the dimerization brings no notable changes onto transient from the ground state to the excited state of dye.

A study of fluorescence of all tested dyes has been performed in both *N*,*N*-dimethylformamide and tetrahydrofurane as solvents at room temperature. Fig. 3 shows the fluorescence spectra for selected bichromophoric dye. All bichromophoric dyes show similar fluorescence characteristic with one broad emission band. The fluorescence data shown in Table 2, suggest that the structure of the acceptor groups (heterocyclic ring) in the molecule is affecting the position of the emission band. As it is shown in Fig. 3 and Table 2, a small red-shift of about 10 nm (270 cm^{-1}) is observed on going from tetrahydrofurane to *N*,*N*-dimethylformamide.

The fluorescence emission spectra bands are somewhat narrower than the absorption spectra (see Table 2). If the broadening of the spectra is understood as deriving from the population of the thermally available conformers, then according to Rettig et al. [28], the observed results can be taken as the evidence that some of these conformers are nonemissive (reduction of the fluorescence band width). The twisting of the olefinic double bonds gives this type conformer. The deactivation of this state should occur mainly by radiationless processes because the energy gap between its excited state and the ground state is very small [29].

Table 3
Reduction and oxidation potential data, energy of the excited state involved in electron-transfer reaction and calculated free energies (ΔG_{el}) of the electron-transfer reaction between the singlet excited state of the dyes and electron donor tested.

Dye	E_{00}[a] [eV]	E_{00}[b] [eV]	E_{red} [V]	ΔG_{el}[a] [kJ × mol^{-1}]	ΔG_{el}[b] [kJ × mol^{-1}]
S5	2.15	2.13	−0.75	−23.16	−21.23
S10	2.15	2.14	−0.76	−18.33	−17.37
O5	2.29	2.27	−0.79	−32.81	−30.88
O10	2.28	2.28	−0.80	−30.88	−30.88
I5	2.13	2.09	−0.85	−11.58	−7.72
I10	2.12	2.11	−0.72	−23.16	−22.19
S1	2.21	2.19	−0.965	−8.20	−6.27
O1	2.33	2.34	−0.425	−71.89	−72.86
I1	2.16	2.4	−0.88	−11.58	−9.65

The oxidation potential of tetramethylammonium *n*-butyltriphenylborate is equal to 1.16 V.
[a] Obtained for THF as a solvent.
[b] Obtained for DMF as a solvent.

Tested dyes represent bichromophoric non-conjugated molecules that show rather small Stokes shift (see Table 2). Nevertheless, such shift indicates that an emitting state is not the Franck–Condon S_1 state reached in the absorption transition but different, the solvent relaxed state, from which the fluorescence originates.

The maxima of emission spectra of dyes in both DMF and THF are located in the range from 559 nm to 665 nm. Emission maxima of homodimeric styryl dyes with long separating link (5 or 10 carbon atoms) are shifted to the long-wave region by up to 323 cm^{-1} relative to the maxima of their parent monomers.

3.3. Electrochemical studies

The previous discussion on solvent-dependent spectroscopic properties of the novel dyes presented here suggests that the energy of singlet state to which electron transfer from the electron donor occurs may be strongly affected by the polarity of the solvent. This, in turn, may have an effect on the value of free energy change for electron transfer process predicted by Rehm–Weller equation [30]. In terms of the practical application of the electron transfer theory to photoinitiated polymerization, we can expect that, the photoinitiation ability of the photoredox pair can be affected by the monomer polarity (besides of its reactivity).

It is well known that the main prerequisite for a PET reaction is that the thermodynamic driving force for the electron-transfer reaction between an excited state of a dye and an electron donor should have a negative value. The free energy of activation (ΔG_{el}) for the PET process can be easily estimated with the Rehm–Weller [30] Eq. (5):

$$\Delta G_{el} = E_{ox}(D/D^{\bullet+}) - E_{red}(A^{\bullet-}/A) - E_{00} - Ze^2/\varepsilon a \quad (5)$$

where: $E_{ox}(D/D^{\bullet+})$ is the oxidation potential of the electron donor, $E_{red}(A^{\bullet-}/A)$ is the reduction potential of the electron acceptor, E_{00} is the energy of the excited state involved in electron-transfer reaction, and $Ze^2/\varepsilon a$ is the Coulombic energy associated with the process. Because, the last term is relatively small in polar or medium polarity media, it can be neglected in the estimation of ΔG_{el}. The oxidation and reduction potentials of both photoredox pair components have been determined from the cyclovoltameric measurements (Table 3).

The electrochemical reduction of the dyes is reversible, as is shown in Fig. 4.

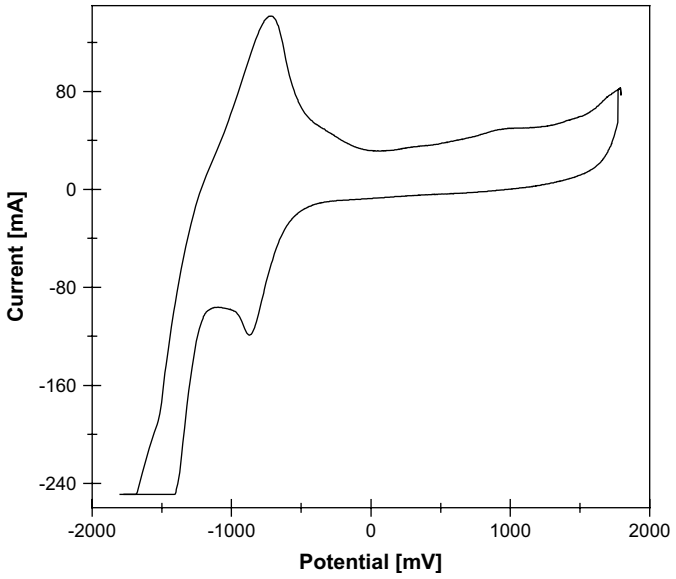

Fig. 4. Cyclic voltammograms of **I10** in 0.1 M tetrabutylammonium perchlorate solution in dry acetonitrile as the supporting electrolyte.

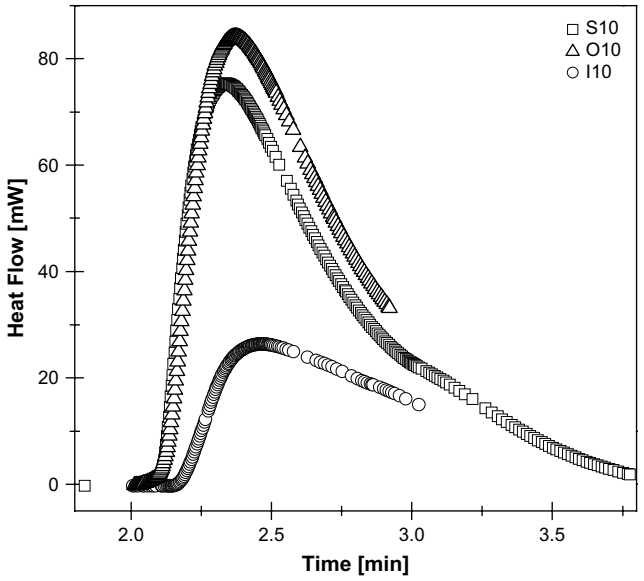

Fig. 5. Family of kinetic curves recorded during the measurements of the flow of heat emitted during the photoinitiated polymerization of the TMPTA/MP (9/1) mixture initiated by bichromophoric styrylcyanine borates marked in the figure. The dye concentration for single chromophore was 2×10^{-3} M and co-initiator concentration was 2×10^{-3} M, respectively. $I_a = 20$ mW/0.196 cm^2. The applied dyes possessed various chromophores and identical borate.

It should be noted that, the oxidation of the tetramethylammonium *n*-butyltriphenylborate is dissociative, and this in turn causes the electrochemical process to be irreversible.

The thermodynamically meaningful oxidation potential can be established with indirect, kinetic method described by Murphy and Schuster [31]. The oxidation potentials measured electrochemically and kinetically differ by about 0.3 V. Therefore, the obtained electrochemical values for both components of photoredox pairs may have only approximate thermodynamic meaning yet, allow us to estimate roughly ΔG_{el} for the PET process.

The measured values of the dye reduction potentials, the electron donor (*n*-butyltriphenylborate anion) oxidation potential (1.16 V), and singlet state energy of the dyes tested allow us to calculate the free energy change for the photoinduced electron transfer process by applying the Rehm–Weller equation [30]. The estimated data are summarized in Table 3.

The values of ΔG_{el} of tested photoinitiating systems oscillate from -32.81 [kJ $\times$ mol^{-1}] to -6.27 [kJ $\times$ mol^{-1}]. The weak polarity dependence of the dyes emission spectra suggests that the energy of singlet state on which electron transfer from an electron donor does not depend on the polarity of an environment. Besides, the calculations clearly show that in monomers of various polarities for almost all tested photoredox pairs the electron transfer process is thermodynamically allowed. This, in turn, allows to predict that the tested dyes in combination with borate anion should effectively generate free radical that can start polymerization of acrylic monomers.

3.4. Photoinitiation – kinetic studies

It is necessary to emphasize that, in order to transfer the styrylcyanine dyes into efficient free radical polymerization initiating system, the exchange of an anion type from iodide on borate anion is needed.

In our studies the photopolymerization initiated by both mono- and bichromophoric styrylcyanine borate salts was performed under irradiation at 514 nm e.g. at the wavelength where the light wavelength is well matched with absorption of dye cations.

The kinetic curves obtained for the photoinitiated polymerization of TMPTA/MP (9:1) mixture recorded for selected styrylcyanine borate salts, under irradiation with a visible light, are shown in Fig. 5 for illustration.

For the comparison of the photoinitiating efficiency Fig. 6 presents the kinetic curves observed for free radical polymerization of TMPTA/MP mixture initiated by both selected mono- and bichromophoric styrylcyanine borates.

Data presented in Fig. 6 show that the polymerization photoinitiation ability of bischromophoric photoinitiating system is close to the photoinitiating ability observed for **RBAX–NPG** couple. It should be emphasized that such high efficiency for tested

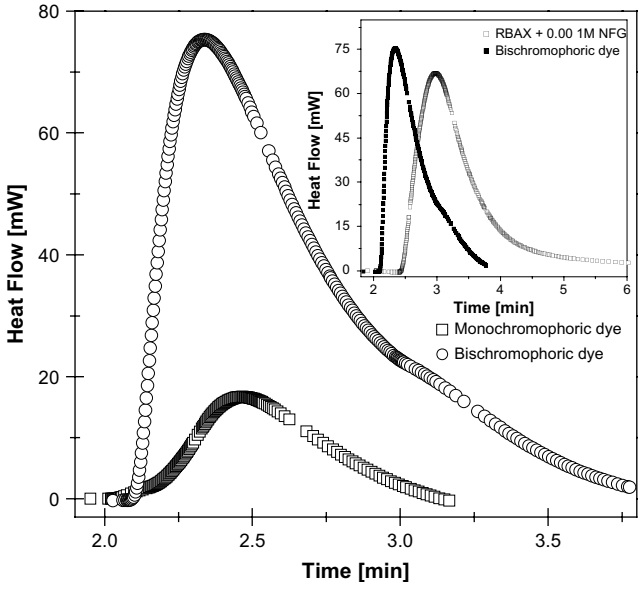

Fig. 6. Family of kinetic curves recorded during the measurements of the flow of heat emitted during the photoinitiated polymerization of the TMPTA/MP (9/1) mixture initiated by mono- and bichromophoric styrylcyanine borates marked in figure. The single chromophore concentrations were 2×10^{-3} M for bichromophoric dye and 5×10^{-3} M for monochromophoric ones, respectively. The co-initiator concentrations were 2×10^{-3} M for bichromophoric dye and 5×10^{-3} M for monochromophoric ones, respectively $I_a = 20$ mW/0.196 cm^2. Inset: Comparison of photoinitiation ability of **RBAX–NPG** (1.0×10^{-3} M) photoinitiating system, **RBAX** – Rose Bengal derivative (triplet state photoinitiator), **NPG** – *N*-phenylglycine and bischromophoric dye.

Table 4
The rate of photoinitiated polymerization and the relative rates of photoinitiation abilities of the styrylcyanine borates tested.

Photoinitiator	R_p [mW/min]	$1 + \ln R_p$ [a.u.]
S5	20.2	2.35
S10	546	5.65
O5	6.92	1.28
O10	438	5.43
I5	22.7	2.47
I10	140	4.29
S1	100.17	3.95
O1	183.38	4.56
I1	5.22	1

photoinitiators is observed when the electron donor concentration is as high as 5×10^{-3} M, e.g. is achieved when the electron donor concentration is five times higher than that present in **RBAX–NPG** pair photoredox pair.

The relative rates of photoinitiated polymerization measured for all the tested photoinitiators are shown in Table 4

It is apparent from the inspection of the initial rates of polymerization that the efficiency of the tested photoinitiators depends strongly on their structure. The highest rates of photoinitiated polymerization were observed for bichromophoric dyes possessing as a spacer a long linking group with 10 carbon atoms between the benzothiazole and benzoxazole rings.

The differences in photoinitiating ability of photoinitiators possessing bichromophoric dyes tested can arise from the structural properties of sensitizers.

It is well known, that the different lengths of linking group are applied to control the distance between two chromophores in dimer molecules. The 3-methylene group is commonly used linkage for most bichromophoric molecules to induce two chromophores to align in a parallel fashion and form an excimer, whereas the 10-methylene group is long enough to make two chromophores separated to individual under relative free condition such as in solution phase [23].

The structural difference between dimers tested is the linkage moiety separating two hemicyanine chromophores. Generally speaking, compared with **S5**, **O5** and **I5**, dyes **S10**, **O10** and **I10** show more similarity to the monomer because the two chromophores in **S10**, **O10** and **I10** are quite well separated from each other. In other words, the hemicyanine chromophores are quite similar to an individual chromophore such as in a case of one-chromophore dyes [24].

From Huang's studies we known that **S5**, **O5** and **I5** molecules can form a folded conformation whose two positive charged chromophores in one molecule are nearly parallel, so called "U-shape" folded molecule. The differences between the photoinitiating ability of photoinitiators composed of bichromophoric dyes possessing 5 and 10 carbon atoms linking group can be caused by: very weak interactions between the two chromophores in one dimer molecule or possibility of formation of excimers after excitation because their chromophores are close to each other [23,24]. However, the results of fluorescence spectra of dyes showed no evidence supporting the occurrence of excimer fluorescence radiation in the longer-wave range (Fig. 3).

The photoinitiator concentration plays a key role in the photopolymerization. In the conventional UV–vis photopolymerization, R_p increases when more initiator is used, however it decreases rapidly if too much initiator is added. This effect is attributed to the "inter-filter effect" and becomes more significant for photoinitiators with high molar extinction coefficient (for tested bichromophoric styrylcyanine borate salt) ε is reaching value about 80 000 M^{-1} cm^{-1}. Fig. 7 presents the relationship between the initial rate of polymerization (taken as the slope of a linear part of kinetic curve at its initial time) and concentration of photoinitiator.

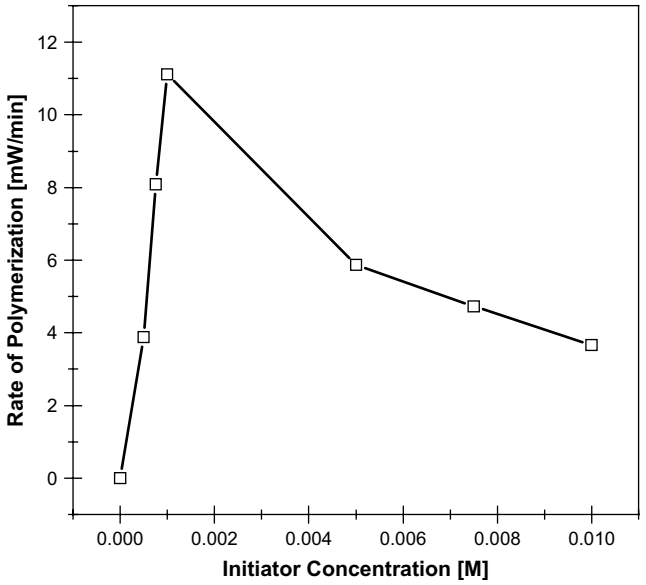

Fig. 7. Rate of polymerization versus photoinitiator concentration (**S5B2**).

It is evident that as the photoinitiator concentration is increasing, the initial rate of polymerization increases and reaches a maximum followed by a continuous mild decrease. For the tested photoinitiator (**S5B2**), the highest rate of polymerization under experimental conditions was achieved at the initiator concentration of about 1×10^{-3} M (single chromophore concentration was 2×10^{-3} M). The reduction of the photoinitiated polymerization rate at higher initiator concentration (for applied technique of polymerization rate measurement) can by easily understood by taking into account the decrease of the penetration depth of the laser beam [32].

The mechanism of photoinitiation, consistent with Schuster et al. [13] observations for cyanine–borate complex has been previously suggested [33]. Electron transfer from the borate anion to the singlet excited state of cyanine dye molecule leads to the formation of cyanine dye radical and boranyl radical which rapidly decomposes producing an alkyl radical. The latter is the most likely initiator of the polymerization of acrylates.

According to Chatterjee et al. studies on symmetrical cyanine borate initiators [14], in non-polar or medium polarity solvents one can treat asymmetric cyanine cation and borate anion as an ion pair. However, studies on the influence of the borate concentration on the rate of photoinitiated polymerization indicate that for identical monomer-dye formulation, a distinct increase in the rate of polymerization is observed as the concentration of borate anion increases [33]. It was previously shown that at the concentration of borate anion equal to the concentration of asymmetric cyanine cation, only a part of the photoredox pairs exists as the ion pair. Only about 20% and 50% for mono- and bichromophoric, respectively, photoredox couples exist as ion pair at the concentration of the dye equal 1×10^{-3} M [16,17,33]. These values give an equilibrium constant equal 3.2×10^{-3} M and 5×10^{-4} M for mono- and bichromophoric dyes, respectively. The differences in both dissociation constants and degree of dissociations seem to be obvious because in the case of the bichromophoric dyes there are two donor molecules in the close proximity to an excited chromophore that causes an increase in the formation of free radical starting polymerization chain reaction.

As it was mentioned above, the electron transfer for cyanine dyes occurs on their singlet state, so the existence of cyanine cation and borate anion as ion pair is the basic prerequisite for the effective electron transfer. Therefore, the additional amount of the

co-initiator should cause an increase of the photoinitiation efficiency. In the case of bichromophoric styrylcyanine dyes, it seems to be obvious that the concentration of electron donor in proximity to each singlet chromophore is increased because of the presence of neighboring second chromophore that couples electron donor. It is also obvious that under continuous laser irradiation (relatively low light intensity) only one chromophore from bichromophoric dye can be excited. Under these circumstances the excited molecule can be quenched by both, its own coupled electron donor or by a donor that is associated with its dimeric partner. Namely, such organization of electron donor artificially increases the concentration of electron donor in proximity to an excited molecule. This, in turn, should substantially increase the rate of singlet excited state quenching, causing in effect, an increase in efficiency of free radical formation. Therefore, the efficiencies of alkyl radical formation and, hence, initiation of polymerization depend on the observed efficiency of electron transfer from the borate anion to the singlet state of cyanine molecule. As it was noted above, the main prerequisite for the electron transfer (PET) reaction, vital for free radical formation, states that the thermodynamic driving force of the electron-transfer reaction between the excited state of the dye cation and *n*-butyltriphenylborate anion should have negative value (see Table 3).

In our earlier papers [34,35] we have shown that in the very viscous media, the rate of polymerization initiated *via* a photoinduced electron transfer can be described as follows:

$$\ln R_p = A - (\lambda + \Delta G_{el})^2 / 8\lambda RT \quad (6)$$

where A for the initial time of polymerization is the sum: $\ln k_p - 0.5\, k_t + 1.5 \ln[M] + 0.5 \ln I_a$ (here k_p, k_t denote the rate constant of polymerization and termination, respectively, [M] is the monomer concentration, I_a is the intensity of absorbed light), λ is the reorganization energy necessary to reach the transition states of both excited molecule and solvent molecules and ΔG_{el} is the free energy change for the photoinduced electron transfer process calculated by applying the Rehm–Weller equation [30].

Eq. (6) clearly indicates that, if the primary process, e.g. the rate of electron transfer process controls the observed rate of photopolymerization, one should observe a parabolic relationship between the logarithm of polymerization rate and the free energy change ΔG_{el} [36].

Fig. 8 presents the logarithm of the TMPTA polymerization rate as a function of the ΔG_{el} value for the initiating systems examined.

It is apparent from the inspection of the relationship presented in Fig. 8 that the plot exhibits predicted by classical Marcus theory of photoinduced electron-transfer reaction [36]. This suggests that at the beginning of the TMPTA polymerization electron transfer process may be the rate-determining step in the radical formation process.

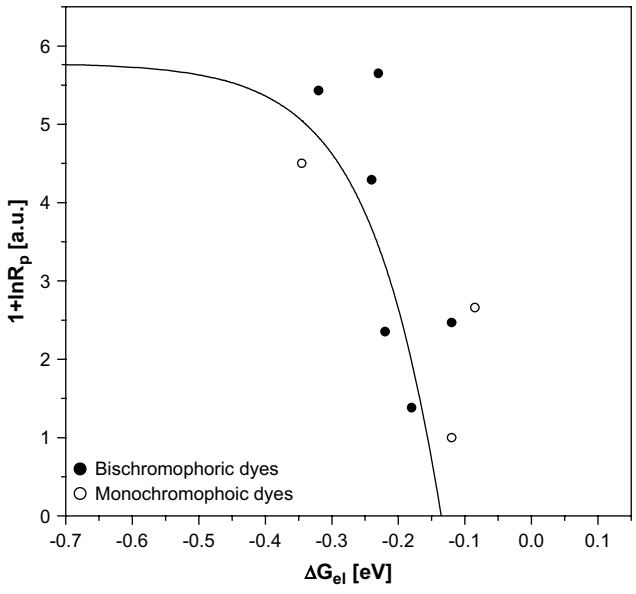

Fig. 8. Rates of polymerization R_p of TMPTA as a function of the free energy change of the electron-transfer reaction from the borate anion to the single excited state of bichromophoric cyanine dyes.

4. Conclusions

A series of styrylcyanine bichromophoric dyes have been synthesized and their steady-state absorption and fluorescence spectra have been investigated. Negative solvatochromic behavior of absorption spectra is observed for all dyes. The analysis of fluorescence spectra in solvents of different polarities indicates the red-shift of the dimers' emission maximum as the solvent polarity increases. Besides, the presented paper is focused on photoinitiation of free radical polymerization initiated by photoreducible dye sensitization.

It was shown that only homodimeric styrylcyanine dyes with linking group possessing of 10 carbon atoms paired with *n*-butyltriphenylborate anion significantly increase the efficiency of photoinitiation of free radical polymerization in comparison to the identical series of monochromophoric styrylcyanine dyes.

Several important conclusions from the experimental data are as follows: (1) The estimated, according the Rehm–Weller equation values of free energy activation for the electron transfer process from an electron donor to the excited electron acceptor show that for the tested photoredox pairs the electron transfer process is thermodynamically allowed (negative values of ΔG_{el}). (2) The rates of polymerization depend on the structure of the dye (The dyes possessing 10 methylene groups linking chain are better photoinitiating systems). (3) Since the rate of polymerization is increased when the thermodynamic driving force of electron transfer process (ΔG_{el}) is increased one concludes that the intermolecular electron transfer process may be the limiting step in the photoinitiated polymerization.

Acknowledgment

This work was supported by The Ministry of Science and Higher Education (MNiSW) (grant No N N204 219734). The authors wish to thank Professor Jerzy Pączkowski for participation in discussion and preparation of the paper.

References

[1] Plambeck LF. US Patent 2,760,863; 1956.
[2] Cohen AB, Walker P. In: Sturge J, Walworth V, Shepp A, editors. Imaging processes and materials. Neblett's 8th ed. New York: Van Nostrand Reinhold; 1989. p. 240.
[3] Neckers DC, Jager W. Photoinitiation for photopolymerization: UV and EB at the millennium. Chichester: John Wiley and Sons; 1998.
[4] Lowe C, Webzter G, Kessel S, McDonald I. Formulation, chemistry and technology for UV and EB formulation for coatings, inks and points. Chichester: John Wiley and Sons; 1997.
[5] Reiser A. Photoreactive polymers: the science and technology of resists. New York: Wiley; 1989.
[6] Monroe BM. Chem Rev 1993;93:435.
[7] Katley AD. J Radiat Curing 1982;3:35.
[8] Eaton F. Pure Appl Chem 1984;56:1191.
[9] Gould R, Shukla D, Giesen D, Farid S. Helv Chim Acta 2001;83:2796–812.
[10] Oster G. Nature 1954;173:300.
[11] Matsumoto S. Bull Chem Soc Jpn 1962;35:1860.
[12] Eaton DF. Photogr Sci Eng 1979;23:150.
[13] Chatterjee S, Davis PD, Gottschalk P, Kurz ME, Sauerwein B, Yang X, et al. J Am Chem Soc 1990;112:6329.

[14] Chatterjee S, Gottschalk P, Davis PD, Schuster GB. J Am Chem Soc 1988; 110:2326.
[15] For examples of cyanine dyes see: (a) Gottschalk P, Neckers DC, Schuster GB. US Patent 4,772,530; 1980 Chem Abstr 1987;107:187434n. US Patent 4,842,980;1988;
(b) Gottschalk P. US Patent 4,874,450; 1989;
(c) Weed G, Monroe BM. US Patent 5,143,818; 1992.
[16] Kabatc J, Jędrzejewska B, Pączkowski J. J Polym Sci Part A Polym Chem 2006;44:6345–59.
[17] Jędrzejewska B, Kabatc J, Pietrzak M, Pączkowski J. J Polym Sci Part A Polym Chem 2002;40:1433–40.
[18] Jędrzejewska B, Jeziórska J, Pączkowski J. J Photochem Photobiol Part A Chem 2008;195:105–10.
[19] Damico R. J Org Chem 1964;29:1971.
[20] Kovalska VB, Kryvorotenko DV, Balanda AO, Losytskyy MYO, Tokar VP, Yarmoluk SM. Dyes Pigm 2005;67:47–54.
[21] Mishra JK, Behera RK, Behera GB. Indian J Chem 2000;39B:783.
[22] Mishra JK, Behera GB, Krishna MMG, Periasamy N. J Fluoresc 2001;92:157.
[23] Huang Y, Cheng T, Li F, Luo C, Huang CH, Cai Z. J Phys Chem B 2002;106:10031–40.
[24] Huang Y, Cheng T, Li F, Luo C, Huang CH, Wang S. J Phys Chem B 2002;106: 10041–50.
[25] Habashy MM, El-Sawawi F, Antonious MS, Sheriff AK, Abdel-Mottaleb MSA. Indian J Chem A 1985;24:908.
[26] Zeena S, Thomas KG. J Am Chem Soc 2001;123:7859.
[27] Lu L, Lachicotte RJ, Penner TL, Peristein J, Whitter DG. J Am Chem Soc 1999;121:8146.
[28] Szczepan M, Rettig W, Bricks YL, Slominski YL, Tolmachev AI. J Photochem Photobiol A 1999;124:75–84.
[29] Wróblewski S, Trzebiatowska K, Jędrzejewska B, Pietrzak M, Gawinecki R, Pączkowski J. J Chem Soc Perkin Trans 2 1999:1909–17.
[30] Rehm D, Weller A. Ber Bunsen Ges Phys Chem 1969;73:834.
[31] Murphy S, Schuster GB. J Phys Chem 1995;99:511.
[32] Zhang S, Li B, Tang L, Wang X, Liu D, Zhou Q. Polymer 2001;42:7575.
[33] Kabatc J, Jędrzejewska B, Pączkowski J. J Polym Sci Part A Polym Chem 2000;38:2365.
[34] Pączkowski J, Kucybała Z. Macromolecules 1995;28:269.
[35] Pączkowski J, Pietrzak M, Kucybała Z. Macromolecules 1996;29:5057.
[36] Marcus RA. J Chem Phys A 1956;24:966.